Climate Risk Management 1 (2014) 25–38

Contents lists available at ScienceDirect

Climate Risk Management

journal homepage: www.elsevier.com/locate/crm

Dynamical seasonal ocean forecasts to aid salmon farm management in a climate hotspot

Claire M. Spillman [a], Alistair J. Hobday [b,*]

[a] Centre for Australian Weather and Climate Research (CAWCR), Bureau of Meteorology, GPO Box 1289, Melbourne, VIC 3001, Australia
[b] Climate Adaptation Flagship, CSIRO Marine and Atmospheric Research, Hobart, TAS 7000, Australia

ARTICLE INFO

Article history:
Available online 9 December 2013

Keywords:
Seasonal forecasting
Climate variability
Climate change
Aquaculture
Atlantic salmon
POAMA

ABSTRACT

Marine aquaculture businesses are subject to a range of environmental conditions that can impact on day to day operations, the health of the farmed species, and overall production. An understanding of future environmental conditions can assist marine resource users plan their activities, minimise risks due to adverse conditions, and maximise opportunities. Short-term farm management is assisted by weather forecasts, but longer term planning may be hampered by an absence of useful climate information at relevant spatial and temporal scales. Here we use dynamical seasonal forecasts to predict water temperatures for south-east Tasmanian Atlantic salmon farm sites several months into the future. High summer temperatures pose a significant risk to production systems of these farms. Based on twenty years of historical validation, the model shows useful skill (i.e., predictive ability) for all months of the year at lead-times of 0–1 months. Model skill is highest when forecasting for winter months, and lowest for December and January predictions. The poorer performance in summer may be due to increased variability due to the convergence of several ocean currents offshore from the salmon farming region. Accuracy of probabilistic forecasts exceeds 80% for all months at lead-time 0 months for the upper tercile (warmest 33% of values) and exceeds 50% at a lead-time of 3 months. This analysis shows that useful information on future ocean conditions up to several months into the future can be provided for the salmon aquaculture industry in this region. Similar forecasting techniques can be applied to other marine industries such as wild fisheries and pond aquaculture in other regions. This future knowledge will enhance environment-related decision making of marine managers and increase industry resilience to climate variability.

Introduction

Aquaculture is seen as an important element in future food security, particularly given projected declines in the availability of wild fish, and the growing human population (Bell et al., 2009; Merino et al., 2012). Future production is uncertain, however, as climate change will further threaten sustainable fisheries and aquaculture production in some regions, while presenting opportunities in others (Brander, 2007; Hobday et al., 2008; Cochrane et al., 2009; Bell et al., 2011). One widely farmed species considered vulnerable to rising ocean temperatures is Atlantic salmon (*Salmo salar*; Battaglene et al., 2008;

* Corresponding author. Tel.: +61 362325310.
E-mail address: alistair.hobday@csiro.au (A.J. Hobday).

2212-0963
http://dx.doi.org/10.1016/j.crm.2013.12.001

Lorentzen, 2008), which is farmed in high latitude coastal waters of both hemispheres (Gross, 1998) and often grown close to its thermal limits.

One important location for salmon aquaculture is Tasmania, Australia. The industry has grown from establishment in 1984 to now represent Australia's most valuable seafood industry (DPIPWE, 2013). It is an important regional employer, worth hundreds of millions of dollars to Tasmania's economy, with additional growth planned for the next decade. Several companies farm salmon in a range of Tasmanian locations; south-east Tasmania accounts for up to 50% of the annual production. Salmon are produced in land-based hatcheries, grown in ponds for 6–12 months, and then moved to coastal sea cages for the final two years of production. While in sea cages, the fish are subject to the local environmental conditions. Fish health and growth are both strongly influenced by ocean temperatures, with salmon in Tasmania grown in waters approaching their upper thermal limit in summer (Battaglene et al., 2008). Under climate change however, thermal tolerances are predicted to be exceeded more frequently, which could lead to degraded fish health, increased disease outbreaks and mortality (Battaglene et al., 2008). This increase in water temperatures is influenced by both general ocean warming, as well as the increased poleward extension of warm water currents from the north (Ridgway, 2007; Wu et al., 2012).

Particularly important for the salmon farms in the south-east of Tasmania, is the seasonal extension of the warm water East Australia Current (EAC). The EAC is a complex and highly energetic western boundary system off eastern Australia and is dominated by a series of mesoscale eddies (Ridgway and Hill, 2009). Flow is strongest in summer, often seen as a tongue of warm water extending south into waters off eastern Tasmania (Ridgway and Godfrey, 1997). South-eastern Australia, including Tasmania, is a climate change 'hotspot' (Hobday and Pecl, 2013). Average temperatures in this region are projected to be 2.8 °C higher than the 1990–2000 average by 2050 (Hobday and Lough, 2011), due in part to the strengthening of the EAC and increased southward flow (Ridgway, 2007). Interannual variability also can also result in warmer than average conditions, and already impacts the industry in some years. Thus, dealing with impacts of a warmer climate is both a current and a long-term challenge for salmon farmers in this region (Hobday et al., 2008).

The Tasmanian salmon industry has identified that coping with climate variability and change can be facilitated with an improved understanding of the marine environment (Battaglene et al., 2008). Advance warning of both extremely warm or cold water temperatures would give farm managers time to respond and adapt management strategies to maximise production (e.g. balanced nutritional requirements) and minimise mortality (e.g. from disease). For the majority of salmon farm managers, information about the future a season ahead is of primary interest, and allows a range of risk management responses to be implemented. Statistical forecasts have been used by the Tasmanian salmon industry in recent years (Hobday et al., 2011b) and whilst these can be skilful, they do not account for a changing climate, or for unprecedented conditions. Given the observed and projected warming trend in this region, reliance on a statistical or climatological approach will be of limited value in the coming years. Dynamical model predictions offer an alternative as there is no assumption of climate stationarity i.e., models can forecast unprecedented events as they are based on physical principles and are not constrained by historical data.

The use of dynamical seasonal forecasting to provide advance warning of ocean conditions for marine management has increased in recent years. The Predictive Ocean Atmosphere Model for Australia (POAMA), developed by the Bureau of Meteorology and CSIRO, is currently used for management purposes in several marine applications. Real-time forecasts for coral bleaching risk on the Great Barrier Reef are currently produced operationally, providing advance warning to reef managers of potential bleaching risk in the upcoming summer (Spillman, 2011a; Spillman et al., 2012). POAMA forecasts of ocean temperature are also combined with a statistical southern bluefin tuna habitat model, to produce tuna habitat maps for the Australian Marine and Fisheries Authority, which are used in setting management zones (Hobday et al., 2011a). In an aquaculture context, a key need is to evaluate if a coupled ocean–atmosphere forecast model such as POAMA can forecast regional ocean conditions at the seasonal time scale, which can then be downscaled to provide information at the coastal farm scale.

The aim of this study is to first assess the regional skill of POAMA in forecasting ocean temperatures in south-east Tasmania and to establish relationships with salmon farm temperatures in the region. We then assess the skill of the model ensemble mean and probabilistic forecasts. The ensemble mean provides the average conditions based on multiple model realisations (ensemble members), while probabilistic forecasts provide information as to the likelihood of an event occurring. Finally, we demonstrate farm-specific forecast products that are delivered to individual salmon farmers to enhance their climate readiness.

Methods

Salmon farm data

Monthly farm temperature data are available for two farms (Huon and Dover) in south-east Tasmania for 1991–2010 (Fig. 1), the longest temperature time series available. The farms are located in waters less than 20 m in depth, and salmon cages are within 500 m from the coast. Water temperatures are measured many times each day using a data logger in a cage at 5 m depth, and supplied as a monthly average for each location. Each dataset has been scaled by removing the long-term monthly mean ocean temperatures for 1991–2010 (i.e., the climatology) for each farm to create temperature anomalies to

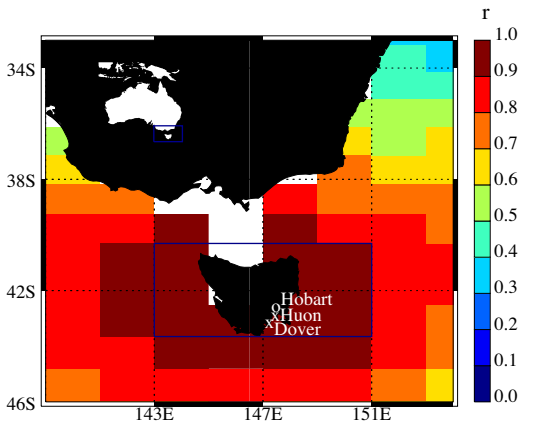

Fig. 1. Spatial correlation (r) of observed ITAS with observed SSTA in south-east Australia. The grid cells plotted indicate the ocean model resolution in the region, where the white grid cells indicate model land cells. Overlaid is the domain (blue box) used to calculate the ITAS index (40.3–43.7°S and 143–151°E). Also shown are the locations of the two focal salmon farm sites, Huon and Dover, and the Tasmanian capital city, Hobart. (For interpretation of the references to colour in this figure legend, the reader is referred to the web version of this article.)

allow for comparison. Temperatures at the two farms are strongly correlated with one other (r = 0.885, p = 0.001, n = 240); on average, the warmest month is February and the coldest month is August.

Model description

POAMA is a global ocean–atmosphere ensemble seasonal forecast system run operationally at the Australian Bureau of Meteorology since 2002. It comprises a coupled ocean–atmosphere model and data assimilation systems for the initialisation of the ocean, land and atmosphere (Spillman and Alves, 2009). The ocean model grid resolution around Tasmania is approximately 200 km east–west and 110 km north–south, with upper vertical layers 15 m deep and increasing with water depth.

A 33 member ensemble of retrospective forecasts (hindcasts) was generated by starting the model (POAMA version 2) 33 times on the first day of each month for 1991–2010, initialised only with data available before the start date and running forward in forecast mode for 4 months. The 33 ensemble members are derived from three separate model configurations of 11 ensembles each (Marshall et al., 2011a). Initial results suggested that there is benefit in creating a multi-model ensemble based on these three different configurations, i.e., errors have different characteristics in each configuration (Langford and Hendon, 2011; Wang et al., 2011).

Initial conditions are provided by two separate data assimilation schemes for POAMA (version 2); an atmosphere/land initialisation system (ALI; Hudson et al., 2011) and an ensemble ocean data assimilation system (PEODAS; Yin et al., 2011a). Perturbed initial conditions, which are required to sample uncertainty in the initial ocean and atmospheric states, are generated using a coupled breeding technique. The coupled breeding produces consistent perturbations to both the ocean and atmosphere at the initial time of the forecasts (for more details see Yin et al., 2011b; Marshall et al., 2011a). Each set of 11 ensemble members within each of the three model configurations are initialised with the resulting 11 different atmosphere and ocean initial conditions.

POAMA monthly modelled SST anomalies (SSTA) were created by removing the model monthly climatology from forecast SST values. The model climatology is the long-term monthly mean ocean temperatures for 1991–2010 to match the farm data time period. The climatology is computed relative to start month and lead-time for the model, and is removed from SST values to reduce the effects of any model bias (Stockdale, 1997). Lead-time is defined as the time elapsed between the model start date (date the model forecast is issued) and the forecast date, i.e., if the start date is 1 February 2010, the monthly forecasts for February, March and April are at lead-times of 0, 1 and 2 months respectively. Generally forecast accuracy is highest for lead-time 0 months and decays as forecasts are made further into the future (i.e., increasing lead-time). Ensemble member forecasts are averaged to give the overall ensemble mean forecast.

A regional Tasmanian SSTA index (ITAS) is calculated by averaging 13 SSTA values over the region 40.3–43.7°S and 143–151°E (Fig. 1, noting white areas are model land cells and are omitted in calculations). The ability for this index to represent the Huon and Dover temperature anomalies and be used as a predictor of farm temperature values is also evaluated. The coarse ocean model grid resolution means that a multi-cell average is a more appropriate indicator of farm conditions than individual grid cell values. The predicted absolute farm temperatures to be delivered to farm operators will consist of the sum of the modelled ITAS value and the observed temperature monthly climatology at each farm.

Model skill

To assess the accuracy of the POAMA temperature forecasts, model skill is calculated by correlating model SSTA ensemble mean values with observed monthly SSTA values in both space and time using the Pearson Correlation Coefficient (Spillman and Alves, 2009). The observed dataset is the PEODAS reanalysis, which assimilates satellite and *in situ* data using a sophisticated pseudo ensemble Kalman filter approach on the ocean model grid (Yin et al., 2011a). To provide a minimum skill baseline for ITAS, persistence forecasts are created using PEODAS by persisting the observed monthly ITAS value from the month immediately prior to each start date over the length of forecast.

In addition to generating correlations, the probabilistic skill of the model is assessed using all 33 ensemble members and cross-validated temperature terciles as appropriate thresholds. To create the tercile thresholds, model and observed values are independently sorted by ascending value. The two points that divide the ordered distribution into three parts each containing a third of the population, are the tercile limits or thresholds. In cross-validation one date is withheld from the dataset and tercile thresholds are generated for the withheld date (Michaelsen, 1987). For a particular forecast, the forecasted tercile is the tercile containing the most ensemble members. In order to determine the accuracy of the forecast system to make predictions for a particular tercile, the forecast hits and correct negatives need to be calculated over the set of hindcasts. For example in assessing the skill of predictions of the upper tercile, if the observed value falls in the upper tercile and the forecasted tercile is in the upper tercile, this counts as a hit. If neither the forecasted tercile nor the observed value fall in the upper tercile, this is deemed a correct negative (Fig. 2). To determine forecast accuracy, forecast hits and correct negatives are summed and divided through by the total number of forecasts for each month and lead-time.

Event counts were generated by counting the number of observation and model grid cells for all ensemble members that fell in each cross-validated tercile, in order to assess whether the model reproduced the correct number, timing and spatial extent of temperature events. Using these counts, Relative Operating Characteristic (ROC) curves were calculated, to assess the useful skill of probabilistic forecasts, with all grid points in the Tasmanian (ITAS) region contributing to the statistics (see Spillman et al., 2011b). The ROC curve is a plot of the hit rate against the false alarm rate and determines the ability of the forecast to discriminate between events and non-events, e.g. falling within or outside a certain tercile (Mason and Graham, 1999). The normalised area under the ROC curve is a useful indicator of skill (a value of 0.5 = no skill, 1 = perfect skill), with a value greater than 0.5 indicating the prediction system has some skill over climatological forecasts (Mason and Graham, 1999).

Results

Observed temperature relationships

The locations of cells that contribute to the ITAS index, together with spatial correlations of observed ITAS with observed SSTA around Tasmania are shown in Fig. 1. The index is strongly correlated ($r > 0.8$) with SSTA around Tasmania and thus is a useful representation of ocean conditions in the region. Observed values for ITAS are plotted against farm temperature anomaly data for Huon and Dover for 1991–2010 in Fig. 3. Values lie close to the diagonal line showing good agreement between the farm and ITAS data, with strong correlations of 0.76 and 0.83 (both statistically significant at $p = 0.001$) for ITAS with Huon and Dover, respectively (Table 1). The ITAS time series and the farm data have similar standard deviations and minimum values, though the magnitudes of peak values at the farms are not always matched by ITAS, particularly at Huon

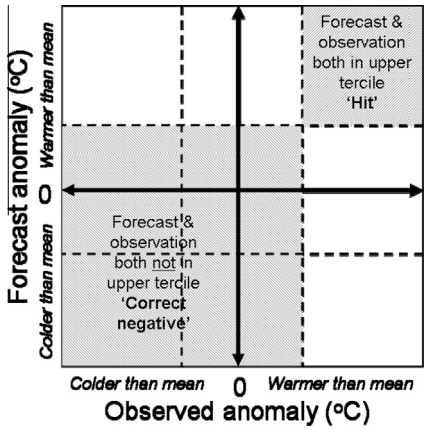

Fig. 2. Contingency table illustrating the definition of hits and correct negatives for the example of an upper tercile. Dashed lines separate the upper, middle and lower terciles.

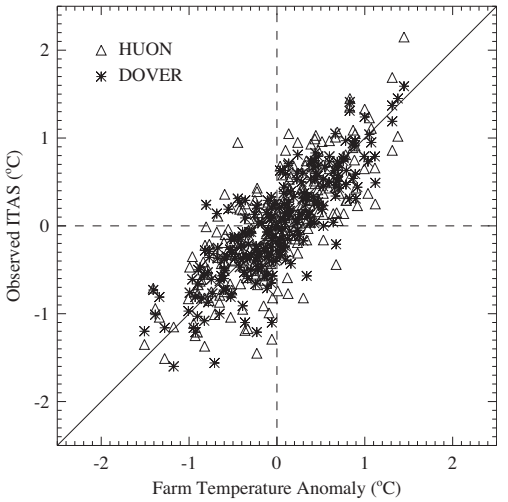

Fig. 3. Monthly observed farm temperature anomalies at Huon and Dover together with observed (PEODAS) ITAS values for 1991–2010.

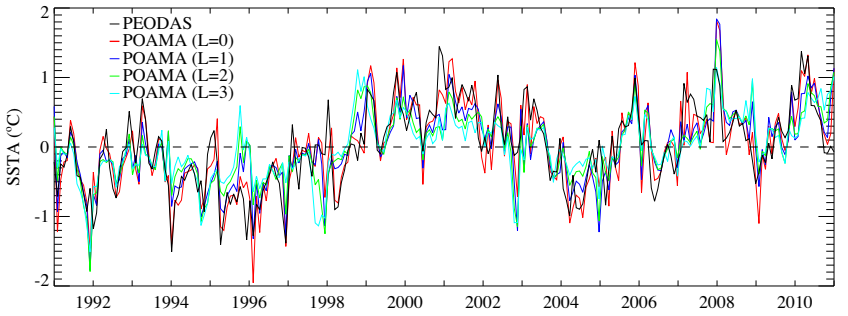

Fig. 4. Observed (PEODAS) ITAS data plotted against model ITAS values for all months 1991–2010 at lead-times (L) 0–3 months.

Table 1
Characteristics of Huon and Dover farm temperature anomaly data and observed ITAS for 1991–2010. Root mean square error (RMSE), normalised RMSE and correlation values of farm data with observed ITAS are also shown for the same period.

	Huon	Dover	ITAS
Maximum value	2.15 °C	1.59 °C	1.45 °C
Minimum value	−1.51 °C	−1.60 °C	−1.51 °C
Standard deviation	0.62 °C	0.59 °C	0.57 °C
RMSE	0.42 °C	0.34 °C	–
Normalised RMSE	11.3%	10.6%	–
Correlation	0.76	0.83	–

(Table 1). The maximum value at Huon was 2.15 °C whereas ITAS peaked at 1.45 °C. The root mean square error (RMSE) values are 0.42 and 0.34 °C for Huon and Dover respectively, and the normalised RMSE is 11% for both sites.

Model skill

The time series of observed monthly ITAS is shown with predicted ITAS ensemble mean values at lead-times 0–3 months for 1991–2010 in Fig. 4. Both predicted and observed (derived from PEODAS) values follow a similar interannual pattern with cooler conditions in the mid 1990s and warm conditions in the early 2000s, although peak ITAS magnitudes are frequently underestimated. There appears to be a weak decadal oscillation evident in the data, possibly linked to changes in the volume of EAC water flowing into southern waters (Hill et al., 2008). The predicted ITAS values match quite well with observed values, though agreement generally decreases with lead-time as predicted peak values often appear to be damped. The model also generally captures the four unusually warm summers in Tasmania – 2001, 2006, 2008 and 2010 (Fig. 4). Conversely,

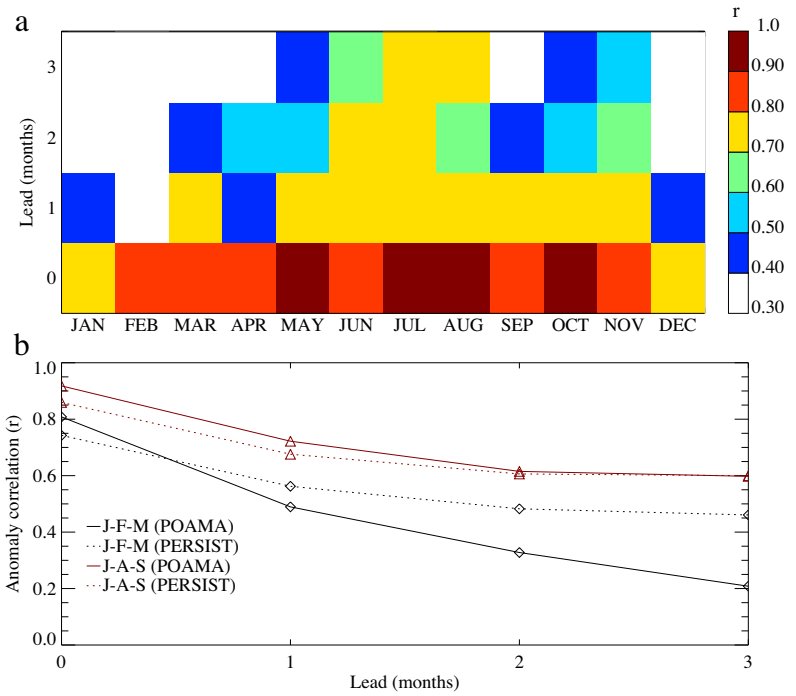

Fig. 5. Anomaly correlations for model ITAS and observed ITAS, together with persistence skill, for (a) each target month and (b) for grouped January–February–March (J–F–M) and July–August–September (J–A–S) target months for 1991–2010. For example, forecasts for target month January at lead-time 3 months are issued 1 October. Persistence forecasts were created using the monthly observed ITAS value of the previous month as the forecast for the next 9 months. In (a) significant correlations are shaded ($r > 0.38$ is significant at $p = 0.1$; t test, $n = 20$).

several peak negative anomalies were predicted to be overly cold by the model at lead-time 0 months, including early 1992, 1996 and 2009. Correlations between observed and predicted values for all months are 0.84, 0.56, 0.45 and 0.35 for lead-times 0, 1, 2 and 3 months, respectively. All are statistically significant at the 99.9% confidence interval ($n = 240$).

The correlations of model ensemble mean ITAS values with observed for 1991–2010 are shown in Fig. 5, together with that of persistence forecasts for ITAS. Anomaly correlations with observed values are above 0.7 for all months at lead-time 0 months and for most months at lead-time 1 month (Fig. 5a), with skill lowest for forecasts for December, January and February at these lead-times. Skill then rapidly declines for both these months ($r < 0.4$) out to lead-times of 2–3 months. Conversely, skill is highest for forecasts for winter months, with skill exceeding 0.7 at a lead-time of 3 months for July (i.e., forecasts issued on 1 April). When compared to persistence skill, model skill is higher for lead-time 0 months but is lower for lead-times of 1–3 months for summer target months January, February and March (J–F–M; Fig. 5b). However for the grouped winter forecast target months, July, August and September (J–A–S), model skill exceeds 0.6 and is higher or equivalent to persistence skill out to 3 months lead-time (Fig. 5b). All correlations in Fig. 5b are statistically significant at the 95% confidence interval ($n = 60$), with the exception of modelled J–F–M at lead-time 3 months. Summer conditions tend to be more variable due to increased EAC activity as shown by a standard deviation for observed ITAS values in summer (J–F–M) of 0.66 whereas in winter months (J–A–S), the standard deviation drops to 0.43. This is also seen in lower persistence skill in summer compared to winter.

Accuracy of the model in correctly forecasting temperatures within the upper and lower terciles respectively is shown for all months at lead-times 0–3 months in Fig. 6. Based on terciles, accuracy must be above 56% to have skill above random chance (Appendix A). Accuracy exceeds 80% for all months at lead-time 0 months for the upper tercile (warmest 33% of values), decaying with lead-time, though values still exceed 50% at lead-time 3 months. For the lower tercile (coldest 33% of values), accuracy again exceeds 80% for most months at lead-time 0 months, with summer (J–F–M) and winter months (J–A–S) exceeding 90%. Accuracy is lowest at lead-time 2–3 months for forecasts for December, January and February.

Probabilistic skill of the model is presented as ROC diagrams, as well as the area under the ROC curve ('A'), for model forecasts of upper tercile in summer target months (J–F–M) and lower tercile in winter target months (J–A–S) in Fig. 7. All cells in the ITAS region were used in calculations (Fig. 1) in order to increase the sample size. A ROC area greater than 0.5 indicates the model has skill, with a value of 1.0 indicating perfect forecasts. Values for both J–F–M and J–A–S for lead-times 0–3 months all exceed 0.5 and so indicate forecasts are more skilful than a climatological forecast. ROC areas are higher for winter months with a very high value of 0.94 for J–A–S at lead 0 months and a value of 0.78 at 3 months lead-time which is equal to the J–F–M value at 1 month lead-time.

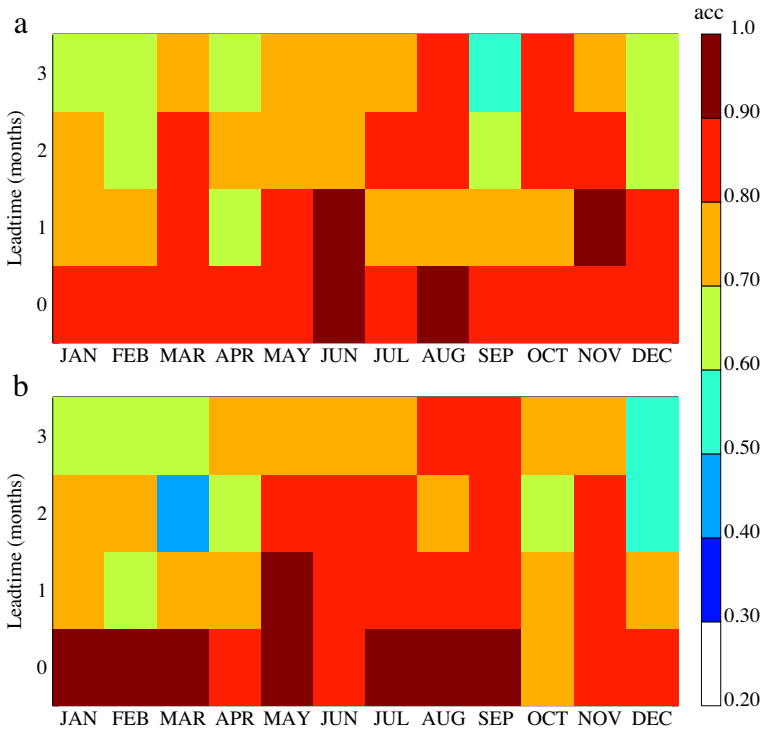

Fig. 6. Accuracy of model ITAS for (a) upper and (b) lower terciles for each target month 1991–2010. Accuracy is the total number of hits and correct negatives divided by total number of forecasts.

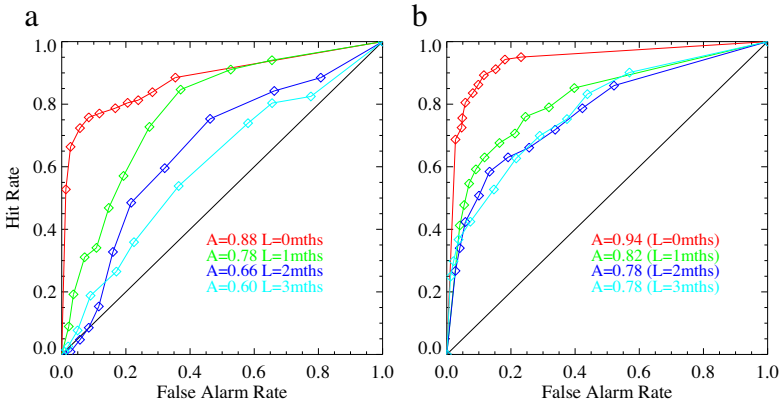

Fig. 7. ROC diagrams and areas ("A") for the ITAS region using all 33 ensemble members and lead-times (L) 0–3 months. (a) Grouped target months January, February and March (J–F–M; summer) for the upper tercile, and (b) target months July, August, September (J–A–S; winter) for the lower tercile.

Forecast delivery

The monthly delivery of forecast information to salmon farmers can take several forms. For example, for experienced forecast users, histograms detailing forecast probability distributions, together with model and observed climatological frequencies, can be used. Example forecasts for Huon for the target dates of February 1996 and November 2000 at lead-times of 0–3 months are presented in Fig. 8. The ensemble spread for each forecast at each lead-time (red bars) indicates the range of possible predicted outcomes for that target date. To provide context for the forecast, both the model (yellow bars) and observed (grey bars) climatologies are also displayed. The model climatology shows the range of anomaly values that the model forecast for that month at that particular lead-time for the period 1991–2010 (n = 20 years × 33 ensembles). The observed climatology likewise shows the distribution of all the observed values for that specific month in 1991–2010 (n = 20 years).

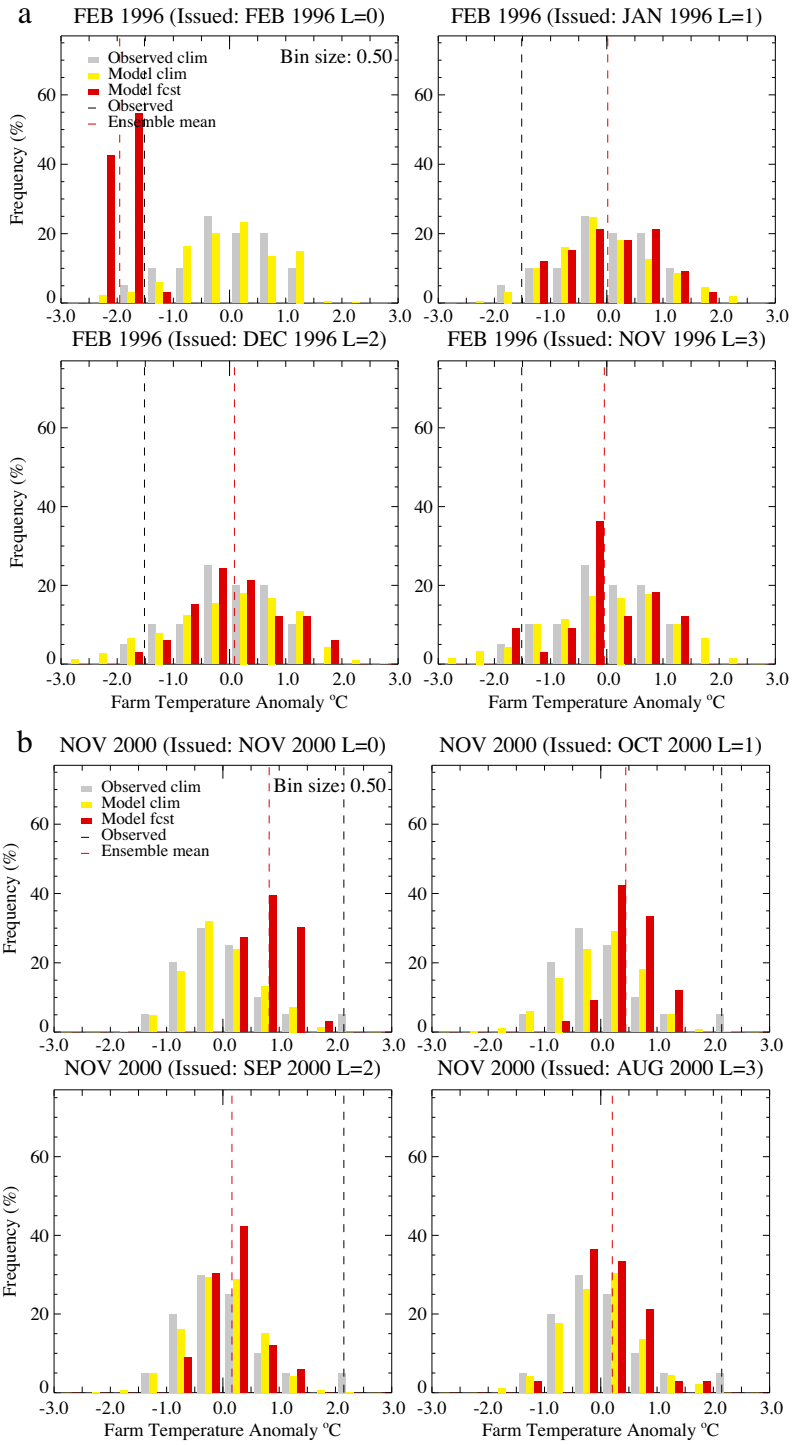

Fig. 8. Example histogram forecast products from the hindcast set for the Huon farm for target dates (a) February 1996 and (b) November 2000. Monthly observed temperature anomaly frequencies are shown in grey bars ($n = 20$ years), model frequency climatology in yellow bars ($n = 20$ years $\times$ 33 ensembles) and the actual forecast frequencies ($n = 33$ ensembles) in red bars. Ensemble mean values are shown as red dashed lines and observed values are shown as black dashed lines. (For interpretation of the references to colour in this figure legend, the reader is referred to the web version of this article.)

Overlaid on each histogram is the observed value (black dashed line) and ensemble mean (red dashed line) for that date. February 1996 was a particularly cold month, with the observed value falling at the lower end of the observed climatological

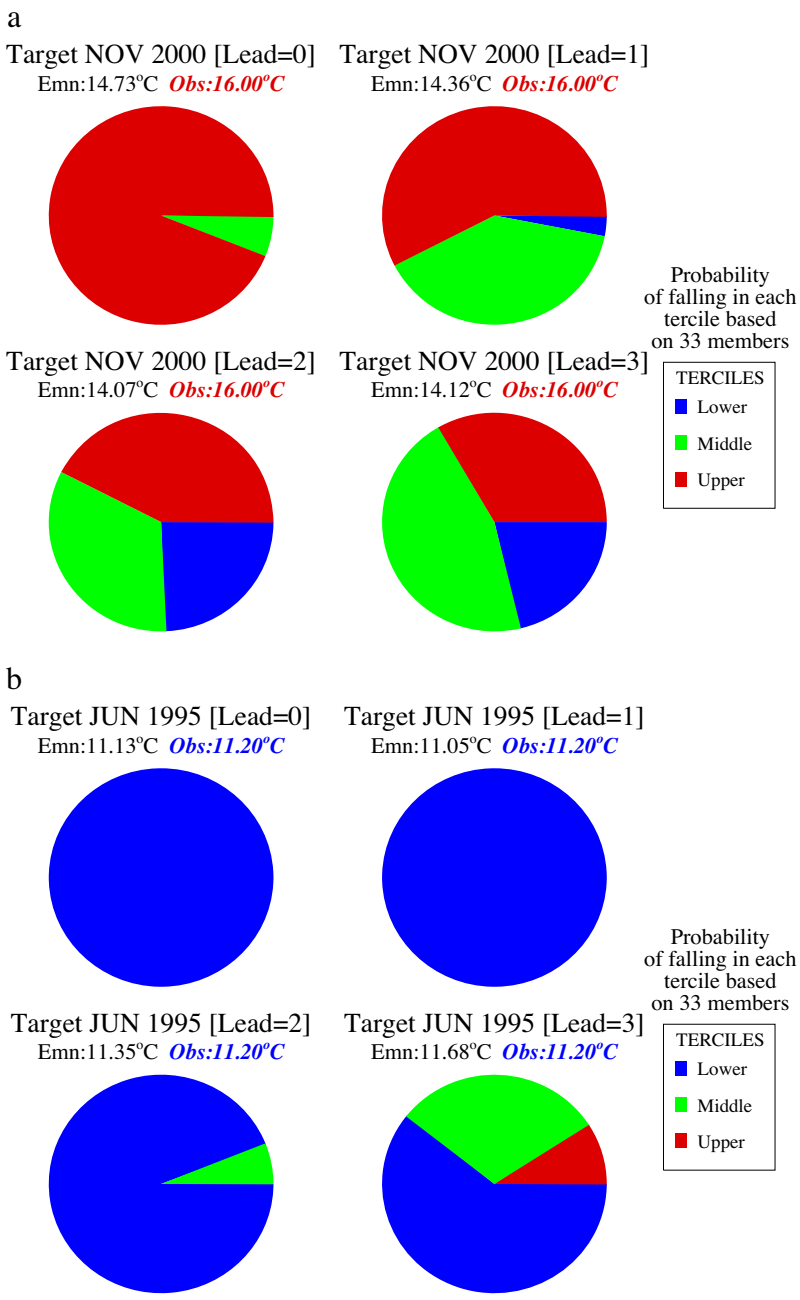

Fig. 9. Example pie chart forecasts products from the hindcast set for the Dover farm for target dates (a) November 2000 and (b) June 1995 at lead-times 0–3 months showing predicted probabilities of temperatures falling in each tercile (red – upper, green – middle, blue – lower). Above each pie chart the ensemble mean value (Emn) is written in black, together with the observed value (Obs) written in the colour of the tercile in which it occurred. (For interpretation of the references to colour in this figure legend, the reader is referred to the web version of this article.)

distribution, with the forecast mean slightly cooler. As lead-times decreased from 3 to 0 months, the ensemble mean value converged to the observed value. For November 2000, the observed farm temperature (black dashed) was extremely warm and towards the maximum value in the observed climatology. Whilst the ensemble mean (red dashed) underestimated the magnitude of the observed value, it approached the observed value as the lead-time decreased. For lead-times 0–1 month, the forecast ensemble distribution was appropriately skewed to the upper end of the model climatology.

In an alternative forecast presentation, based on pie charts and terciles, we show example retrospective forecasts for two target dates November 2000 and June 1995 for Dover at 0–3 months lead-time (Fig. 9). Each colour used in the pie charts depicts the proportion of the 33 ensemble members which fall in a particular tercile category. November 2000 was a particularly warm month with an observed temperature of 16.0 °C which was in the upper tercile, i.e., within the warmest

33% of values recorded for 1991–2010. Model ensemble members fell predominantly in the upper tercile at a lead-time of 0 and 1 month. Ensemble mean values were slightly colder than the observed value. Conversely June 1995 was an especially cold month with an observed temperature of 11.2 °C falling in the lower tercile. Over 75% of the model ensemble members indicated the lower tercile up to 4 months ahead, thus predicting this cold event. The forecast ensemble mean temperature was within 0.56 °C of the observed value at all lead-times.

In real-time delivery mode, we provide forecasts for the coming months from a given start date. As these are forecasts, monthly climatological values are shown for reference rather than observed values, which are unavailable. Again the colours used in the pie charts depict the fraction of ensemble members that fall within each tercile category. Examples of operational

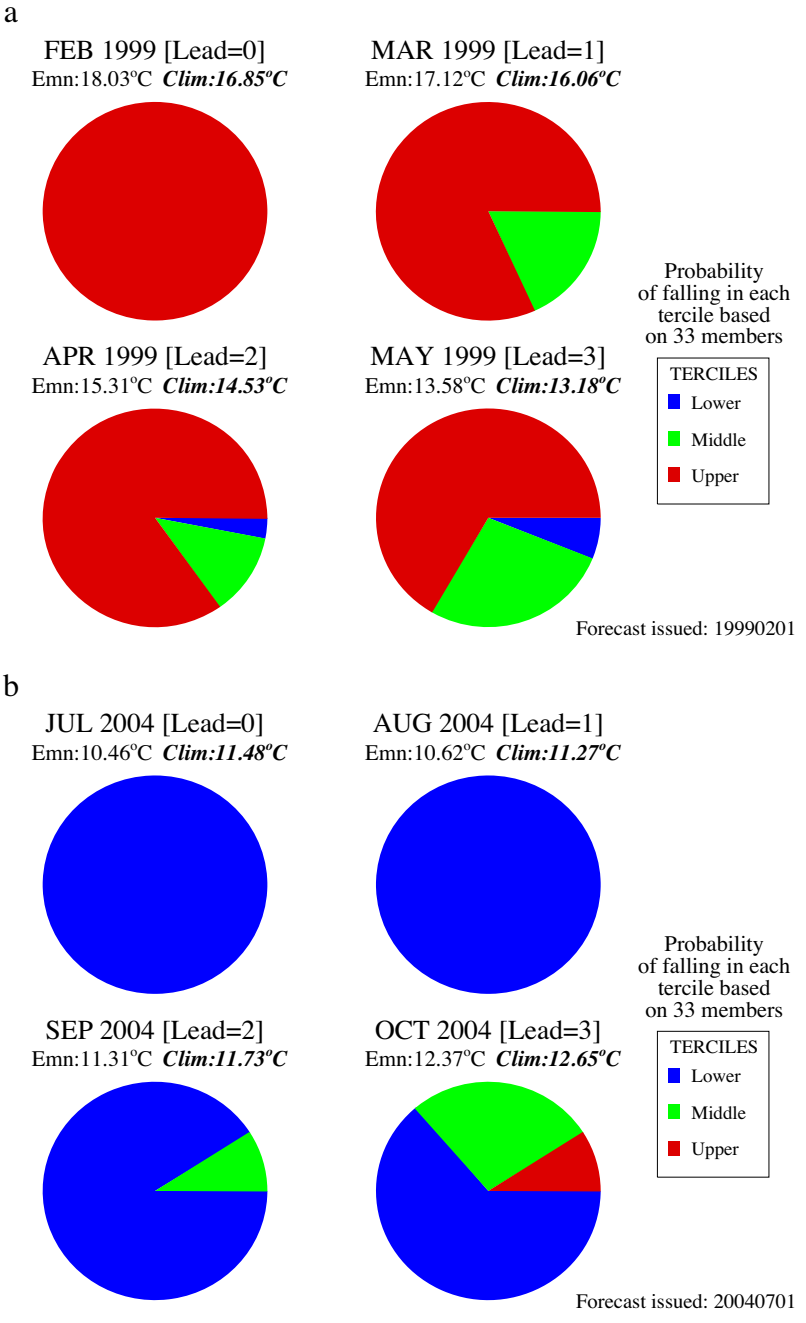

Fig. 10. Example operational pie chart forecast products for Dover for forecast start dates (a) February 1999 and (b) July 2004 for lead-times 0–3 months showing predicted probabilities of temperatures falling in each tercile (red – upper, green – middle, blue – lower). Above each pie chart the ensemble mean value (Emn) is written in black with the monthly climatological (Clim) value shown for reference. (For interpretation of the references to colour in this figure legend, the reader is referred to the web version of this article.)

real-time forecast pie charts for Dover are shown in Fig. 10 for the start dates February 1999 and July 2004 for the following 4 months. For the forecast starting 1 February 1999, the subsequent 4 months are all projected to be warmer than usual, with the highest proportion of ensemble members falling in the upper tercile (red). For months March, April and May, despite up to a third of ensemble members indicating cooler conditions, the ensemble mean values consistently exceed monthly climatological values, indicating to the salmon farmers that warmer conditions are expected for the coming months. For the forecast beginning 1 July 2004, the upcoming months are predicted to be colder than usual, particularly July and August where 100% of forecasts fall in the lower tercile. For October the ensemble mean value is below the climatological mean, as the majority of ensembles are in the lower tercile, indicating to the salmon farmers that a cool period is approaching.

Discussion

Forecasts of ocean conditions can be used to better prepare salmon farm managers for expected environmental conditions and can increase their resilience to extremes. As for many other primary industries, aquaculture farm managers need to know the likelihood of particular conditions in the upcoming season, and see this as more relevant than climate projections for the upcoming decades (Battaglene et al., 2008; Hobday et al., 2011b; Spillman et al., 2011a). A challenge in providing forecasts for coastal users has been the potential mismatch in spatial scales of the forecast models and local environmental conditions. We have shown here that useful local forecasts are possible for salmon farms in south-east Tasmania.

Users need to have confidence in forecasts in order to use them to inform management decisions, so extensive validation is critical in developing that confidence. A strong relationship between observed farm temperatures and average ocean conditions (ITAS index) around Tasmania was found over the period 1991–2010. Despite farms generally being located within relatively sheltered coastal waters, temperatures were strongly influenced by the adjacent ocean and regional atmospheric processes. In general terms, if ocean conditions around Tasmania are warmer than normal, farm temperatures are also generally warmer.

Predictions of salmon farm temperatures, using regional ocean forecasts from POAMA and a simple statistical analysis, have been shown to be skilful at up to 3 months lead-time. The model adequately captures the regional oceanographic features around Tasmania and the ITAS index is representative of the region. Anomaly correlations for predicted ITAS were above 0.3 for all months at lead-times with the exception of December, January and February at lead-times 2–3 months (Fig. 5). In summer therefore, a hybrid forecast approach, combining persistence and model forecasts, may be more skilful, and deserves further exploration. Skill for winter months beat persistence at all lead-times, whereas for summer months, persistence was higher than the model at lead-times of 1–3 months. However, accuracy in forecasting whether temperatures will fall in the upper tercile in summer or lower tercile in winter was up to 90% at lead-time 0 months and exceeded 60% at lead-time 3 months for all months except December and January, above the random threshold of 56%. ROC scores for upper and lower terciles in summer and winter respectively exceeded 0.5 for all lead-times, indicating that based on all these indicators, the model has useful skill, and skill exceeding that of climatological forecasts.

Model skill was generally higher in winter than summer months for all measures used. Persistence skill is also comparatively high in winter months, suggesting that variability is lower and oceanographic features persist longer than in summer months. Higher variability in summer months may be due to the EAC extending further southward as a series of warm water eddies along the east coast of Australia (Ridgway, 2007). The resolution of POAMA is too coarse to resolve eddies, which may explain the poorer skill in summer months. Furthermore, the model often underestimated the magnitude of the observed ITAS values, particularly at longer lead-times (Fig. 4). Again this may be due to the coarse resolution of the ocean model. Bass Strait is absent from the ocean model as Tasmania is approximated as a land bridge attached to mainland Australia (Fig. 1) which would have implications for regional oceanography. Additionally, Hobday et al. (2011b) found that the best correlation of summer farm water temperatures is with February mean air temperature in Hobart (a city some 80 km distant). This implies that a contributing factor determining farm temperatures is atmospheric processes. However, the Tasmanian landmass does not exist in the atmospheric model component of POAMA which may also limit model skill in the region.

The model generally captured the warm summer events of 2001, 2006, 2008, and 2010, during which La Niña events occurred. Ridgway et al. (2008) showed a weak correlation between the EAC and El Niño-Southern Oscillation (ENSO) events such as La Niña. Observed correlations of ITAS in February and July with the mean SSTA in the equatorial NINO4 region [5°N–5°S, 160°E–140°W] of the previous December for 1982–2010 are low and negative (−0.14, −0.34 respectively). However, correlations of observed ITAS in February with observed global SST anomalies for the same period showed a strong correlation with SST on the north-west shelf of Western Australia ($r > 0.6$, data not shown) in the preceding November. Heat content in this region has also been linked to strength of the Leeuwin Current (Tomczak and Godfrey, 1994; Hendon and Wang, 2010). The Leeuwin Current is a south flowing current along the Western Australian coast, transporting warm low-saline tropical waters down the coast across the Great Australian Bight, with peak strength in winter months (Ridgway and Condie, 2004). Volume transport by the Leeuwin Current is dominated by ENSO and is greater during La Niña years (Feng et al., 2003). The Leeuwin Current extension along Australia's south coasts may contribute warmer water to the ITAS region in summer (Ridgway and Condie, 2004).

Evaluation studies and feedback exercises regarding forecast presentation and dissemination conducted in land-based agricultural industries have identified several important considerations when designing seasonal forecast products for use by industry (e.g. Marshall et al., 2011b). A good understanding of the end user skills and what they need the forecast

products for is essential. Information on relevant spatial and temporal scales as well as the minimum level of skill or accuracy of forecasts in the target region in the season of question required is necessary. The importance of social factors in forecast use has also been emphasised (Marshall et al., 2011b). The types of management decisions that would be made depending on a particular forecasted outcome and what threshold initiates management actions also need to be considered. For example, must the forecast indicate 90% certainty of an outcome before action is taken or is a probability of 60% sufficient?

In this study we presented probabilistic forecasts two different ways i.e., as histograms and as pie charts. The pie chart format may be easier for users to understand using the analogy of a loaded roulette wheel – the odds of the roulette ball landing in any one of the terciles depends on the forecast probabilities. It is also important to liaise with users and incorporate feedback into product design to maximise usefulness. We are presently working with salmon companies to evaluate the desired delivery model and to evaluate the benefits of the management options they implement in response to the forecasts (Hobday et al., 2011b). Some potential management strategies that can be implemented in response to these seasonal forecasts include planning for freshwater bathing to reduce disease in warm summers, organising staff rosters based on expected management needs, thinning salmon populations and shifting pens to cooler locations to combat the impacts of extreme temperature conditions. Adoption and use of seasonal forecast tools over a period of time is more likely to result in long term benefit, as opposed to adoption for a single season or cycle. It is also important to ensure users take a long term view, as forecasts can and will be incorrect in some situations (Marshall et al., 2011b). Ongoing education in the use of these tools is very important so that managers can understand both the strengths and limitations of forecast products and the best way to interpret forecasts (e.g. Spillman et al., 2011a). Future versions of POAMA will include finer model grid spacing, with better resolution of Tasmania and Bass Strait, providing more regional detail with higher skill.

Overall, seasonal forecasts for marine users can encourage proactive management, rather than reactive management, improving business resilience under both climate variability and long-term change. Marine industries are increasingly aware that climate change may bring both opportunities on which they could capitalise and impacts against which they need to increase their resilience (Hobday et al., 2008; Hobday and Poloczanska, 2010; Spillman et al., 2011a). These types of forecast tools can be used in other marine management applications in different regions including coral reefs, wild fisheries and other aquaculture industries (e.g. Hobday et al., 2011a; Spillman, 2011a,2011b), and can help businesses learn in real-time on the job, providing immediate benefits in terms of managing risk under climate variability. In the longer term, food security is predicted to be a serious concern under climate change and so better management of fishery and aquaculture resources to improve resilience is essential (Bell et al., 2011; Merino et al., 2012). Armed with these tools and understanding, the Tasmanian salmon industry will be well placed to implement a number of adaptation strategies at seasonal time scales that will reduce their exposure to warm water events as they adapt to long-term change in this fast warming region.

Acknowledgements

The authors acknowledge project funding from Tasmanian Salmonid Growers Association, Australia and thank Faina Tseitkin, Griffith Young and Guo Liu (Bureau of Meteorology, Australia) for preparing the model hindcasts. Thanks to reviewers Dr Rich Little (CSIRO) and Drs Lynda Chambers, Oscar Alves and Debbie Hudson (all of Bureau of Meteorology) for their review of previous versions of the manuscript.

Appendix A. Calculation of expected probability of random events based on terciles

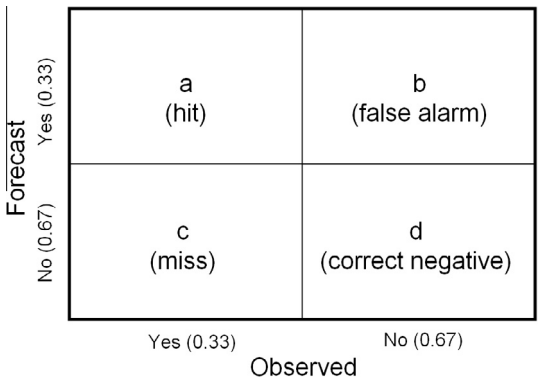

The probability of a "yes" is 0.33, and a no is 0.67.

Thus, accuracy, *A* is the probability of a correct "yes" forecast by chance plus the probability of "no" forecast by chance. Multiplying the marginal probabilities;

$$A = \left(\frac{a+b}{n}\right)\left(\frac{a+c}{n}\right) + \left(\frac{c+d}{n}\right)\left(\frac{b+d}{n}\right)$$

where n = total number of forecasts, assumed to be independent events (Sokal and Rohlf, 2012) Thus,

$$A = (0.33 \times 0.33) + (0.67 \times 0.67)$$

$$A = 0.56$$

A.1. Reference

Sokal, R.R., Rohlf, F.J., 2012. Biometry: The Principles and Practice of Statistics in Biological Research, third ed. W.H. Freeman and Co., New York, p. 937.

References

Battaglene, S,. Carter, C., Hobday, A.J., Lyne, V., Nowak, B. 2008. Scoping study into adaptation of the Tasmanian Salmonid Aquaculture Industry to potential impacts of climate change. National Agriculture & Climate Change Action Plan: Implementation Programme report, p. 83. Available at: <http://www.imas.utas.edu.au/right-column-content/publications-search?queries_publication_type_query=Research+Reports>.

Bell, J.D., Kronen, M., Vunisea, A., Nash, W.J., Keeble, G., Demmke, A., Pontifex, S., Andrefouet, S., 2009. Planning the use of fish for food security in the Pacific. Mar Policy 33, 64–76.

Bell, J.D., Johnson, J.E., Hobday, A.J. (Eds.), 2011. Vulnerability of Tropical Pacific Fisheries and Aquaculture to Climate Change. Secretariat of the Pacific Community, Noumea, New Caledonia.

Brander, K.M., 2007. Climate change and food security special feature: global fish production and climate change. PNAS 104, 19709–19714.

Cochrane, K., De Young, C., Soto, D., Bahri, T. (Eds.), 2009. Climate change implications for fisheries and aquaculture: overview of current scientific knowledge. FAO Fisheries and Aquaculture Technical Paper. No. 530, Rome, FAO, p. 212.

DPIPWE, 2013. Tasmanian Seafood Industry Scorecard 2011–12. Available at: <http://www.dpiw.tas.gov.au/inter,nsf/WebPages/CART-76FVXV?open>.

Feng, M., Meyers, G., Pearce, A., Wijffels, S., 2003. Annual and interannual variations of the Leeuwin Current at 32 S. J. Geophys. Res. 108, 33–55.

Gross, M.R., 1998. One species with two biologies: Atlantic salmon (*Salmo salar*) in the wild and in aquaculture. Can. J. Fish Aquat. Sci. 55, 131–144.

Hendon, H.H., Wang, G., 2010. Seasonal prediction of the Leeuwin Current using the POAMA dynamical seasonal forecast model. Clim. Dyn. 34, 1129–1137.

Hill, K.L., Rintoul, S.R., Coleman, R., Ridgway, K.R., 2008. Wind forced low frequency variability of the East Australia Current. Geophys. Res. Lett. 35, L08602.

Hobday, A.J., Hartog, J.R., Spillman, C.M., Alves, O., 2011a. Seasonal forecasting of tuna habitat for dynamic spatial management. Can. J. Fish Aquat. Sci. 68, 898–911.

Hobday, A.J., Lough, J.M., 2011. Projected climate change in Australian marine and freshwater environments. Mar. Freshw. Res. 62, 1000–1014.

Hobday, A.J., Lyne, V., Thresher, R., Spillman, C., Norman-Lopez, A., 2011b. Atlantic Salmon aquaculture subprogram: forecasting ocean temperatures for salmon at the farm site, FRDC report 2010/217.

Hobday, A.J., Poloczanska, E.S., 2010. Fisheries and aquaculture. In: Stokes, C.J., Howden, S.M. (Eds.), Adapting Agriculture to Climate Change: Preparing Australian Agriculture, Forestry and Fisheries for the Future. CSIRO Publishing, Melbourne.

Hobday, A.J., Poloczanska, E.S., Matear, R., 2008. Implications of climate change for Australian fisheries and aquaculture: a preliminary assessment. Report to the Department of Climate Change, Canberra, Australia. August 2008. Available from: <http://www.cmar.csiro.au/climateimpacts/reports.htm>.

Hobday, A.J., Pecl, G.T., 2013. Identification of global marine hotspots: sentinels for change and vanguards for adaptation. Rev. Fish Biol. Fish.. http://dx.doi.org/10.1007/s11160-013-9326-6.

Hudson, D.A., Alves, O., Wang, G., Hendon, H.H., 2011. The impact of atmospheric initialisation on seasonal prediction of tropical Pacific SST. Clim. Dyn. 36, 1155–1171.

Langford, S., Hendon, H., 2011. Assessment of international seasonal rainfall forecasts for Australia and the benefit of multi-model ensembles for improving reliability, CAWCR Tech. Rep. 39:33. ISBN: 978-1-921826-57-3 (PDF/Electronic Resource).

Lorentzen, T., 2008. Modeling climate change and the effect on the Norwegian salmon farming industry. Nat. Resour. Model. 21, 416–435.

Marshall, A.G., Hudson, D., Wheeler, M.C., Hendon, H.H., Alves, O., 2011a. Evaluating key drivers of Australian intra-seasonal climate variability in POAMA-2: a progress report. CAWCR Res. Lett. 7, 10–16.

Marshall, N.A., Gordon, I.J., Ash, A.J., 2011b. The reluctance of resource-users to adopt seasonal climate forecasts to enhance resilience to climate variability on the rangelands. Climate Change Econ. 107, 511–529.

Mason, S.J., Graham, N.E., 1999. Conditional probabilities, relative operating characteristics, and relative operating levels. Weather Forecast 14, 713–725.

Merino, G., Barange, M., Blanchard, J.L., Harle, J., Holmes, R., Allen, I., Allison, E.H., Badjeck, M.-C., Dulvey, N.K., Holt, J., Jennings, S., Mullon, C., Rodwell, L.D., 2012. Can marine fisheries and aquaculture meet fish demand from a growing human population in a changing climate? Global Environ. Change 22, 795–806.

Michaelsen, J., 1987. Cross-validation in statistical climate forecast models. J. Clim. Appl. Meteorol. 26, 1589–1600.

Ridgway, K.R., 2007. Long-term trend and decadal variability of the southward penetration of the East Australian Current. Geophys. Res. Lett. 34, L13613.

Ridgway, K.R., Condie, S.A., 2004. The 5500-km-long boundary flow off western and southern Australia. J. Geophys. Res. 109, C04017.

Ridgway, K.R., Godfrey, J.S., 1997. Seasonal cycle of the East Australian Current. J. Geophys. Res. 102 (22), 921–22,936.

Ridgway, K.R., Coleman, R.C., Bailey, R.J., Sutton, P., 2008. Decadal variability of East Australian Current transport inferred from repeated high-density XBT transects, a CTD survey and satellite altimetry. J. Geophys. Res. 113, C08039.

Ridgway, K., Hill, K., 2009. The East Australian Current. In: Poloczanska, E.S., Hobday, A.J., Richardson, A.J. (Eds.), A Marine Climate Change Impacts and Adaptation Report card for Australia 2009. NCCARF Publication 05/09, ISBN 978-1-921609-03-9.

Spillman, C.M., 2011a. Operational real-time seasonal forecasts for coral reef management. J. Oper. Oceanogr. 4, 13–22.

Spillman, C.M., 2011b. Advances in forecasting coral bleaching conditions for reef management. Bull. Am. Meteorl. Soc. 92, 1586–1591.

Spillman, C.M., Alves, O., 2009. Dynamical seasonal prediction of summer sea surface temperatures in the Great Barrier Reef. Coral Reefs 28, 197–206.

Spillman, C.M., Alves, O., Hudson, D.A., 2012. Predicting thermal stress for coral bleaching in the Great Barrier Reef using a coupled ocean-atmosphere seasonal forecast model. Int. J. Climatol.. http://dx.doi.org/10.1002/joc.3486.

Spillman, C.M., Alves, O., Hudson, D.A., Hobday, A.J., Hartog, J.R., 2011a. Using dynamical seasonal forecasts in marine management. In: Chan, F., Marinova, D., Anderssen, R.S., (Eds.), MODSIM2011, 19th International Congress on Modelling and Simulation. Modelling and Simulation Society of Australia and New Zealand, December 2011.

Spillman, C.M., Alves, O., Hudson, D.A., 2011b. Seasonal prediction of thermal stress accumulation for coral bleaching in the tropical oceans. Mon. Weather Rev. 139, 317–331.

Stockdale, T.N., 1997. Coupled ocean–atmosphere forecasts in the presence of climate drift. Mon. Weather Rev. 125, 809–818.

Tomczak, M., Godfrey, J.S., 1994. Regional Oceanography: An Introduction. Pergamon, London.

Wang, G., Hudson, D., Yin, Y., Alves, O., Hendon, H., Langford, S., Liu, G., Tseitkin, F., 2011. POAMA-2 SST skill assessment and beyond. CAWCR Res. Lett. 6, 40–46.

Wu, L., Cai, W., Zhang, L., Nakamura, H., Timmermann, A., Joyce, T., McPhaden, M., Alexander, M.A., Qiu, B., Visbeck, M., Chang, P., Giese, B., 2012. Enhanced warming over the global subtropical western boundary currents. Nat. Clim. Change 2, 161–166.

Yin, Y., Alves, O., Oke, P.R., 2011a. An ensemble ocean data assimilation system for seasonal prediction. Mon. Weather Rev. 139, 786–808.

Yin, Y., Alves, O., Hudson, D., 2011b. Coupled ensemble initialization for a new intraseasonal forecast system using POAMA at the Bureau of Meteorology. IUGG conference, International Union of Geodesy and Geophysics Conference (IUGG), Melbourne, 28 June-7 July.